The Journal of Experimental Biology 213, 2284-2293

doi:10.1242/jeb.041806

The effects of turbulent eddies on the stability and critical swimming speed of creek chub (*Semotilus atromaculatus*)

H. M. Tritico[1,*] and A. J. Cotel[2]

[1]Youngstown State University, 1 University Plaza, Youngstown, OH 44555, USA and [2]University of Michigan, 2340 GG Brown Building, Ann Arbor, MI 48109, USA

*Author for correspondence (hmtritico@ysu.edu)

Accepted 22 March 2010

SUMMARY

The effect of turbulent eddy diameter, vorticity and orientation on the 2 min critical swimming speed and stability of creek chub (*Semotilus atromaculatus*) is reported. Turbulent eddies were visualized and their properties were quantified using particle image velocimetry (PIV). Flow fields with an increasing range in eddy diameter were created by inserting cylinder arrays upstream from the swimming test section. Eddy vorticity increased with increasing velocity. Two orientations of eddies, eddies spinning about a vertical axis and eddies spinning about a horizontal (wall-to-wall) axis, were investigated. Stability challenges were not observed until the largest (95th percentile) eddy diameters reached 76% of the fish body total length. Under these conditions fish were observed to spin in an orientation consistent with the rotational axis of the large eddies and translate downstream. These losses in postural control were termed 'spills'. Spills were 230% more frequent and lasted 24% longer in turbulent flow fields dominated by horizontal eddies than by vertical eddies of the same diameter. The onset of spills coincided with a 10% and 22% reduction in critical swimming speed in turbulent flows dominated by large vertical and horizontal eddies, respectively. These observations confirm predictions by Pavlov et al., Cada and Odeh, Lupandin, and Liao that the eddy diameter, vorticity and orientation play an important role in the swimming capacity of fishes.

Key words: creek chub, critical swimming speed, eddies, stability, swimming, turbulence.

INTRODUCTION

Turbulence is ubiquitous in natural flow environments. While there is not yet a consensus on a single definition of turbulence (Tennekes and Lumley, 1972; Roshko, 1976), it has been shown to affect gamete dispersal (Montgomery et al., 1996), food availability (Mackenzie et al., 1994; Mackenzie and Kiorboe, 1995; Mackenzie and Kiorboe, 2000; Landry et al., 1995), individual energy budgets (Standen et al., 2002; Standen et al., 2004; Enders et al., 2003) and habitat selection (Pavlov et al., 2000; Smith et al., 2005; Cotel et al., 2006) of fishes. A turbulent flow, for the purpose of this paper, is taken as flow which is composed of a continuum of eddies (Tennekes and Lumley, 1972; Cimbala et al., 1988). This definition of turbulent flow acknowledges the fact that the temporal unsteadiness commonly measured in rivers (Nikora and Goring, 1998; Tritico and Hotchkiss, 2005; Smith et al., 2005; Cotel et al., 2006) is primarily due to eddies (rotating packets of fluid). Further, it acknowledges that the most common flow experienced by fish in a fluvial environment is composed of a distribution of eddy sizes, vorticity and orientations (Standen et al., 2002). Incorporating a distribution of eddies complicates the flow beyond current models which assume the flow to be rectilinear [most critical swimming speed studies (e.g. Webb et al., 1984)] or composed of a single eddy diameter (Lupandin, 2005; Liao et al., 2003).

Several researchers have proposed that eddy diameter, vorticity and orientation relative to the fish should be important in understanding the effects of turbulence on fish swimming performance (Pavlov et al., 2000; Cada and Odeh, 2001; Nikora et al., 2003; Biggs et al., 2005; Lupandin, 2005; Tritico and Hotchkiss, 2005; Liao, 2007), with diameter, vorticity and orientation of eddies being primary variables. This idea remains untested. The purpose of this paper is therefore to describe the effects that turbulent eddy diameter, vorticity and orientation have on the critical swimming speed and stability of creek chub.

MATERIALS AND METHODS

Changes in fish swimming performance were measured at several flow speeds and levels of turbulence induced by upstream cylinder arrays of differing diameters and orientations. The turbulent flow regimes were measured using particle image velocimetry (PIV) and were characterized according to eddy composition with eddies being described by eddy diameter (d_e), eddy vorticity (ω_e) and eddy orientation (vertical or horizontal). The spatial preference of fish in the eddy field, the speed at which fish first lost control of posture and location (first spill), spill location, spill frequencies, the method of recovery and critical swimming speed were recorded on video and quantified.

Apparatus

Observations of fish swimming behavior were made during increasing velocity tests in an Engineering Laboratory Design (Lake City, MN, USA) flow visualization water tunnel (Fig. 1) with an observation chamber 250 cm in length and 60 cm wide. The water depth was held at 55 cm for all tests. A 30 cm test section was delineated within the observation chamber by a downstream grid (1.25 cm egg crate) and upstream by either a similar grid or one of three cylinder arrays spanning the flume cross-section. Arrays were composed of cylinders with diameters of 0.4 cm, 1.6 cm and 8.9 cm, with gaps equal to cylinder diameter in each array. Each of these three cylinder arrays could be installed in the flume with either a horizontal orientation (cylinders spanned from left to right wall) or

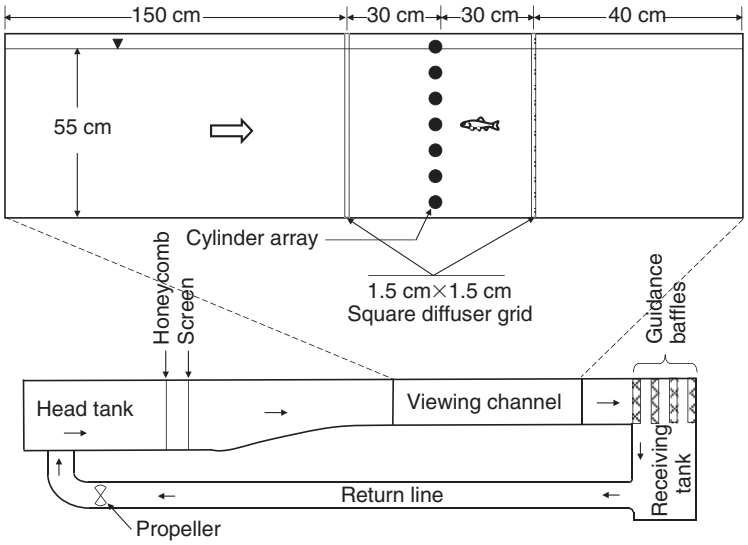

Fig. 1. Flume and test section configuration. Water is recirculated using a variable speed pump; arrows show the direction of flow. A 30 cm long test section was delineated upstream by a cylinder array and downstream by a square diffuser grid. The test section was therefore 60 cm wide×55 cm water deep and 180 cm from the viewing channel entrance. Both the flume (lower drawing) and viewing channel (upper drawing) are portrayed as side views.

vertical orientation (cylinders spanned from bed to free surface). Therefore there were seven treatments: control (1.25 cm egg crate), small horizontal (SH), small vertical (SV), medium horizontal (MH), medium vertical (MV), large horizontal (LH) and large vertical (LV) arrays. A 1.3 cm mesh of 0.04 cm diameter plastic thread was attached to the upstream side of the cylinders to prevent fish escaping. One wall of the observation chamber was lined with 2 cm×2 cm black and white checkered paper to foster fish station holding. All edges of the test sections were electrified at 5 V DC to encourage swimming in a fully turbulent environment. Fish swam away from the walls in a controlled manner and performance did not appear to be affected by the presence of the electrical field along the wall.

Flow analysis

Instantaneous flow patterns were recorded using two-dimensional PIV for depth-averaged velocities, $\bar{u}$, of 8.5, 17.1, 27.7, 38.7 and 50.2 cm s^{-1}. These velocities represent the slowest speed and every third velocity increment that the fish experienced. Analysis of turbulence parameters at these five velocities captured both the range and the trends of turbulent eddy characteristics that the fish experienced. The pulse separations between laser pulses for each of the previous flow speeds were of 8, 5, 3, 2 and 1 ms, respectively. The pulse separation was chosen such that the average particle displacement between image pairs was less than a quarter of the cross-correlation window size (Westerweel et al., 1997; Tritico et al., 2007). The chosen pulse separations correspond to particle displacements that are approximately one-eighth the cross-correlation window size and minimized the number of outlier pixels and ultimately incorrect velocity vectors and turbulence statistics. The water was seeded with 1 μm diameter neutrally buoyant titanium dioxide particles, at a concentration of 1.2 p.p.m. Flow was illuminated using a 120 mJ NdYAG dual-head 532 nm pulsed laser (Gemini-PIV, NewWave, Fremont, CA, USA) with a pulse duration of 100 μs, creating a laser sheet 0.75 mm thick spanning the test section either horizontally (for vertical cylinder arrays) or vertically (for horizontal cylinder arrays). Fifty image pairs were recorded at each flow speed. Each group of 50 image pairs captured an average of 12 eddy shedding cycles from the cylinders.

Downstream from the horizontal cylinder arrays a vertical laser sheet was positioned along the flume centerline. The interrogation window was 26 cm in the streamwise direction and 30 cm in the vertical direction, beginning 2 cm from the bed, downstream grid and upstream cylinders. This 2 cm buffer not only avoided light reflections associated with edges but also kept the flow data consistent with the fish behavior data, as fish behavior was not recorded if the fish was within 2 cm of any edge. Particle displacements, and therefore eddies, were analyzed within the bottom 50% of the flume in order to avoid stray air bubbles in the upper part of the water column. These would have produced erroneous results due to cross-correlation analyses tracking bubble paths rather than the neutrally buoyant flow particles. Downstream from the vertical cylinder arrays, the interrogation window in the horizontal laser sheet was centered on the flume centerline, halfway between the bed and the free surface (Fig. 2). During turbulence data collection (not when fish were swimming in the flume), a 0.9 mm thick black metal sheet was placed directly below the water surface to optically mask the surface waves created by the vertical cylinder arrays. The flow region affected by the presence of this plate was calculated to be restricted to a 1.5 cm region whereas the velocity measurements were collected 25 cm from the plate.

Flow was reconstructed from pairs of images of the particles as recorded by a 1 mega pixel, 10 bit, 30 frames s^{-1} Uniq Vision (Santa Clara, CA, USA) black and white CCD camera driven by PixelFlow software (Huang et al., 1997; Gharib and Dabiri, 2000; General Pixels, 2000; Tritico et al., 2007).

Eddies were identified following the method described by Drucker and Lauder (Drucker and Lauder, 1999). Cross-correlation techniques were used to convert consecutive images of particles into velocity vector fields. The vorticity (ω, twice the angular velocity) was calculated from the velocity vector field. Each local minimum and maximum vorticity within a vorticity field was taken as an eddy center following Drucker and Lauder (Drucker and Lauder, 1999). The circulation about each eddy center was calculated in concentric circles until a maximum circulation (Γ_e – angular momentum per unit mass) was reached:

$$\Gamma_e = \omega_e \times a_e , \quad (1)$$

where a_e is the area circumscribed by the circle ($\pi d_e^2/4$) and ω_e is the spatially averaged vorticity within the circle. The diameter with maximum circulation was taken to be the eddy diameter (Drucker and Lauder, 1999; Wilga and Lauder, 1999); each eddy's location, diameter and average vorticity were recorded.

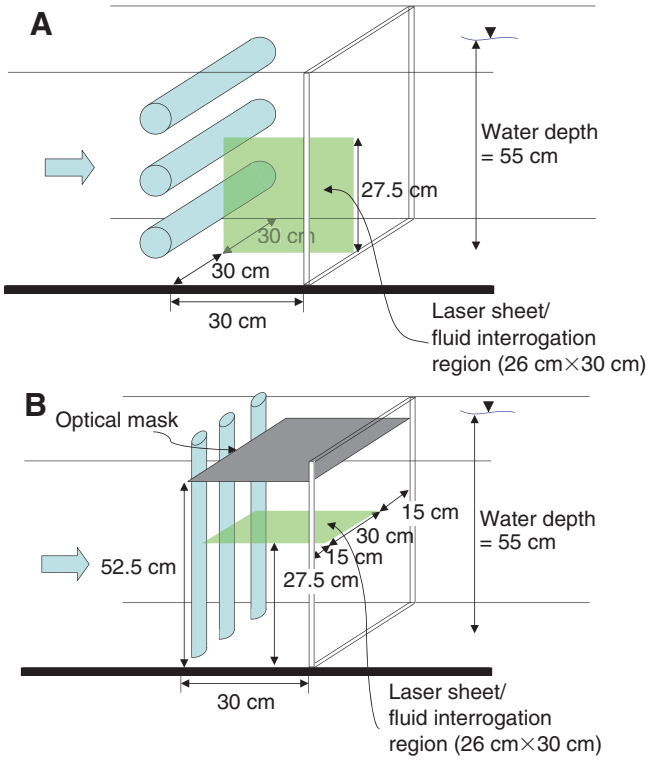

Fig. 2. Location of particle image velocimetry (PIV) interrogation windows. (A) Horizontal cylinder – the green square indicates the laser sheet. (B) Vertical cylinder – the laser sheet is now horizontal and a black sheet metal optical mask was placed 2.5 cm below the water surface to remove background water surface reflection from the PIV images.

Because turbulent flows downstream of sources develop over space and time, the flow in the test section downstream from the control and the six cylinder treatments was originally subdivided into three streamwise regions. Each streamwise region was approximately equal to the fish body length. Moderate streamwise variations in eddy diameter and vorticity were recorded. These variations compared well with previous observations (Zhang and Zhou, 2001; Zdravkovich, 2003; Akilli et al., 2004) of flow downstream from cylinder arrays. However, the greatest variation in both flow metrics and fish behavior occurred as a result of (a) the cylinder diameter and (b) the transverse position in the flow with respect to the large cylinders (Figs 7 and 11). Therefore, for the sake of brevity, the streamwise variations in flow and fish behavior have been omitted from this paper. A detailed discussion of streamwise results has been presented previously (Tritico, 2009).

Fish were observed swimming throughout the water column in the control, small diameter and medium diameter cylinder array treatments without choosing locations relative to the cylinders. In contrast, fish regularly chose various swimming locations relative to the large cylinders. Therefore, flow was analyzed for three cross-flow regions for the large cylinder array. These locations were classified as (a) the large cylinder area directly downstream from each large cylinder (cylinder centerline ± 2.3 cm), (b) the large edge area directly downstream from each cylinder edge (cylinder edge ± 2.3 cm), and (c) the large gap area directly downstream from each gap between the cylinders (gap centerline ± 2.3 cm).

Fish

Creek chub (*Semotilus atromaculatus* Mitchill 1818) were obtained using a Smith-Root (Vancouver, WA, USA) model 15-D backpack electroshocker from Fleming Creek, MI, USA, at a water temperature of 21.1°C. Fish were acclimated in the lab to room temperature (20.5±0.4°C) for at least one week prior to the experiment and were fed goldfish flake food to satiation daily. The experimental temperature was the same as the acclimation temperature. Seven creek chub with an average total length of 12.2±0.9 cm (mean ± 2 s.e.m.) and mass of 16.8±3.5 g were used in these experiments. Each fish was swum with every treatment. The order of the treatment for the fishes was randomized and fish were given a minimum of 3.5 days to recover between each test.

A single fish was placed in the observation section and acclimated to a $\bar{u}$ of 8.5 cm s^{-1}. After 11 h of acclimation, $\bar{u}$ was increased by 3.5 cm s^{-1} increments at 2 min intervals until the fish became entrained on the downstream grid for 3 s. Depth-averaged velocity values that the fish could experience (depending upon the velocity at which fish were entrained) were therefore: 8.5, 11.4, 14.3, 17.1, 20.6, 24.1, 27.7, 31.4, 35.1, 38.7, 42.5, 46.3 and 50.2 cm s^{-1}. The velocity increments used in critical swimming speed tests vary across investigation (Farlinger and Beamish, 1977) depending upon the stated goal of the test. In this investigation the goal of the critical swimming speed test was twofold. The first was to provide a reproducible measure of swimming ability between turbulence treatments. The second goal was to achieve a wide range of speeds (and therefore turbulence conditions) for both video analysis and PIV measurements. The velocity step of 3.5 cm s^{-1} followed the method laid out by Webb (Webb, 1998) and succeeded in providing both a means for general comparison between turbulence treatments and a wide range in flow conditions. The 2 min critical swimming speed was calculated as:

$$2\,\text{min}\; u_{\text{crit}} = \bar{u}_{\text{p}} + \Delta\bar{u} \times \Delta t / 2\,, \qquad (2)$$

where $\bar{u}_{\text{p}}$ is the cross-sectionally averaged flow speed prior to fatigue and Δt is the time in minutes that the fish was able to sustain the highest cross-sectionally averaged flow speed (Brett, 1963).

Fish were continuously videotaped at 30 frames s^{-1} simultaneously from the side and from below using two digital video cameras (Panasonic Model No. PV-DV601D, Kadoma, Osaka, Japan). Fish moved about the test section, holding position for variable periods at various locations. Swimming kinematics were measured from video records when fish remained in a given location with no postural changes for >5 s, during which time fish velocity varied by <0.02 body lengths s^{-1} (Wilga and Lauder, 2002).

In the presence of large cylinders fish suddenly lost the ability to control posture and hold position. The head rotated more than 45 deg and the body was displaced downstream >0.5 of the stretched-straight body length. These events were described as 'spills' and indicated that control of posture and swimming trajectory was overwhelmed. Fish recovered from a spill by reorienting the body axis to the mean flow direction and holding position in the flow with no additional translation downstream. Each spill and recovery was analyzed frame-by-frame to determine the kinematics of the spill, the recovery and the overall duration. Additionally, the test section location in which each spill occurred was recorded and compared with the percentage of time spent at the location. The fish's location in the test section was marked at 5 s intervals for each treatment and speed. Smaller time intervals were tested but no significant difference in results was found. The amount of time that a fish spent in a given flow region was divided by the total treatment time to calculate the percentage of time spent in a given flow region.

Turbulence regimes

Biological flumes and low-turbulence flumes are not free from turbulence (Brett, 1963; Farlinger and Beamish, 1977; Enders et

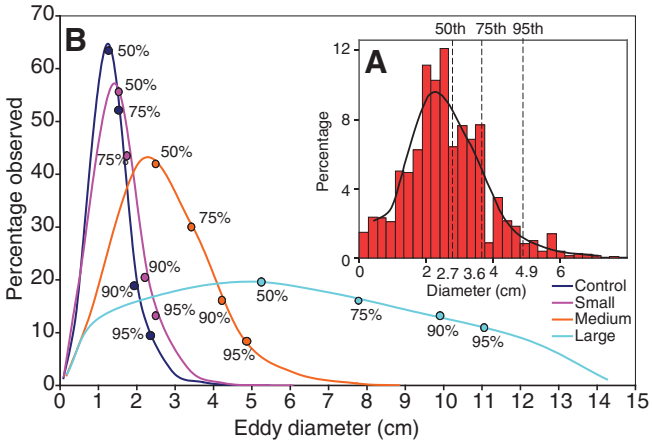

Fig. 3. The distribution of eddy diameters varied across cylinder treatment. (A) Example histogram for flow in the medium horizontal cylinder treatment at a depth-averaged velocity, $\bar{u}$, of 27.7 cm s^{-1} showing the location of the 50th, 75th and 95th percentile eddy. (B) The eddy distributions across cylinder treatment. The proportion of large eddies (with respect to the 12.2 cm fish length) is increased with increasing cylinder diameter. The labeled dots represent the eddy percentile.

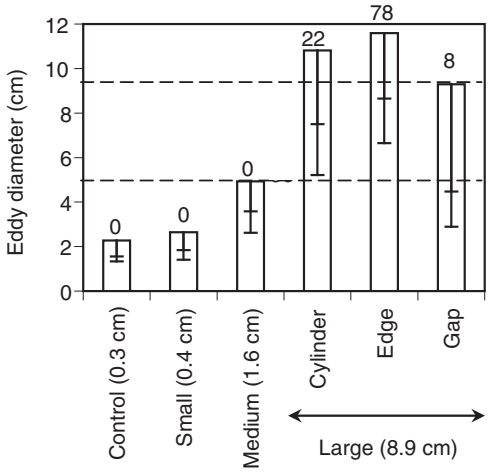

Fig. 4. The 95th percentile eddy diameter varied across treatment and flow region. Eddy diameter increased with cylinder diameter (cylinder diameters are listed in parentheses). For the large cylinders, eddy diameter was largest within the large edge region and smallest within the large gap region. The number of spills observed in each flow regime is listed above each bar. Each bar represents the 95th percentile eddy value while the whiskers represent the 50th and 75th percentiles.

al., 2003), and the biological requirement of delimiting the upstream end of observation sections to avoid fish escape introduces additional turbulence. Hence the production of small isotropic turbulent eddies was unavoidable in the control and all treatments but the range of eddy diameters was increased by the treatments.

Turbulent flow regimes are composed of a range of turbulent eddy diameters (von Karman, 1937; Taylor, 1938; Batchelor and Townsend, 1947). The distribution of eddy diameters tends to be positively skewed, with a large number of small eddies and relatively few large diameter eddies (Fig. 3). This positively skewed distribution pattern was found for all treatments in these experiments (Fig. 3B). Several researchers (Cada and Odeh, 2001; Nikora et al., 2003; Biggs et al., 2005; Lupandin, 2005) have predicted that it is the relatively large/infrequent eddies in most flow distributions that have the greatest potential to perturb a fish when these are of similar size to the length of a fish. For this reason, the cylinder treatments were designed to increase the proportion of large eddies in the flow up to eddy diameters approaching the fish length (Fig. 3B).

Fish spills, which indicate the loss of control over posture and location, also occurred infrequently, suggesting that infrequent but large eddies in the flow indeed had the greatest impact on the fish. No spills were observed for fish swimming in the medium cylinder treatment where the 95th percentile eddy was 4.9 cm, while eight spills were observed within the large gap flow region where the 95th percentile eddy was 9.3 cm (Fig. 4). Therefore, in order to focus the results and discussion on the largest eddies, eddy characteristics for the 95th percentile eddies are reported for each treatment. The median (50th percentile) and the 75th percentile eddy characteristics are also included in figures in order to give a more complete picture of the flow in each treatment. While the magnitudes of the eddy variables were different, the trends across flow regime and general conclusions were similar irrespective of whether the 50th, 75th or 95th percentile eddy was analyzed.

RESULTS

The presence of obstructions created local flow variations. The local velocities, u_{local}, measured by PIV were equal to $\bar{u}$ (<±3%) from the flume system curve in all tests for the control, small cylinder and medium cylinder arrays and in the large edge region of the large cylinders. The flume system curve is the relationship, determined by the flume manufacturer (Engineering Laboratory Design), of the water speed in the test section as a function of the pump speed. In the gap between cylinders (large gap) u_{local} was on average 53% greater than $\bar{u}$ while directly behind the cylinders (large cylinder) u_{local} was on average 38% less than $\bar{u}$ (Fig. 5).

The eddy diameter increased with cylinder diameter for all speeds; the small, medium and large cylinder arrays producing 95th

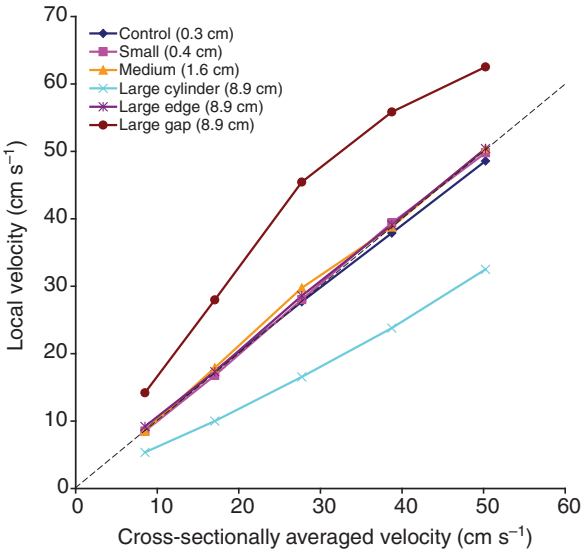

Fig. 5. A comparison of local velocity u_{local} with cross-sectionally averaged velocity $\bar{u}$ for flow regions and treatment. The u_{local} within the test section has been plotted and matched to $\bar{u}$ for all control, small cylinder, medium cylinder and large edge treatments. The u_{local} in the large cylinder region increased at a lesser rate than $\bar{u}$ while the u_{local} in the large gap region increased at a greater rate than the $\bar{u}$. The cylinder diameter is listed in parentheses after each treatment in the figure. The dashed line represents perfect agreement between the pump system curve and the local velocity.

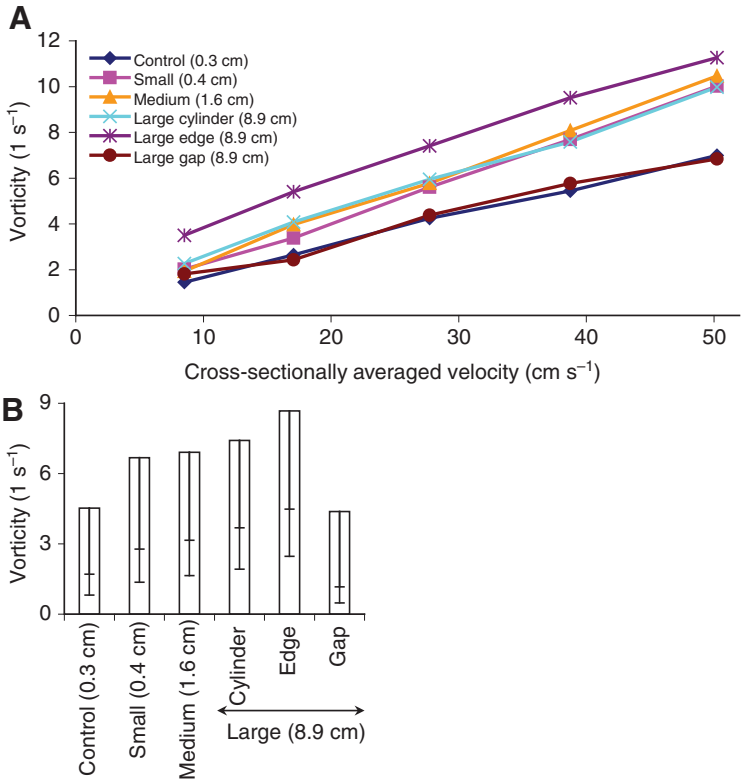

Fig. 6. The 95th percentile eddy vorticity varied across treatment and flow region. (A) Eddy vorticity by $\bar{u}$. Eddy vorticity increased linearly with $\bar{u}$. (B) Eddy vorticity increased with cylinder diameter (diameters are shown in parentheses), and for the large cylinders vorticity was greatest in the large edge region and least within the large gap region. Each bar represent the rapidly rotating eddies (95th percentile) while the whiskers represent the 50th and 75th percentiles. Data in B are for an exemplary speed of 27.7 cm s^{-1}.

percentile eddy diameters of 2.6, 4.9 and 11.2 cm, respectively (Fig. 4). As expected, because the shear-layer eddies are shed and convected through the edge regime of the flow, the largest eddies are found in the large edge regime (95th percentile eddy diameter=11.6 cm). The 95th percentile eddy vorticity increased linearly with $\bar{u}$ (Fig. 6A) and increased with cylinder diameter (Fig. 6B). The large edge regime is the location where the shear-layer eddies are shed, and through which most shear-layer eddies are conveyed. As such, at an exemplary $\bar{u}$ of 27.7 cm s^{-1} vorticity in the large edge regime was 7.4 s^{-1}, greater than the vorticity of 4.5, 5.6 and 5.8 s^{-1} in the control, small cylinder and medium cylinder treatments and also greater than the vorticity of 5.9 and 4.4 s^{-1} in the large cylinder and large gap regions. Conversely, the large gap regime consisted of relatively high speed rectilinear flow that was infrequently entrained by shear-layer eddies. This area, therefore, had similar vorticity to that of the control treatment.

Location preference

While fish moved freely about the test section, they were found at a higher frequency in some regions than in others (Fig. 7). At low speeds fish spent the most time, 73%, in the gap flow region and spent the least amount of time, 7%, in the cylinder flow region (P<0.05 ANCOVA with transverse locations, treatment, $\bar{u}$ and interaction terms). As speed increased, fish in the LH treatment moved to the cylinder region while fish in the LV treatment moved to the edge region (Fig. 7). At the lowest speeds, where swimming required relatively little power, fish chose a regime with higher velocity but smaller diameter turbulent eddies and lower vorticity (Figs 4 and 5, Fig. 6B, Fig. 7) than surrounding regions. As speed increased, fish appeared to be using the turbulent wakes or recirculation zones as time-averaged velocity shelters (Fig. 5). However, station holding (maintaining position for greater than 5 s) in the wake occurred less frequently indicating that these areas were not ideal refuges. The observation that the fish used the edge regions of the LV cylinder array treatment more frequently than in the LH cylinder array treatment indicates that the fish were better able to control posture and location with the large, high vorticity vertical eddies found in the edge zone (Fig. 4 and Fig. 6B) rather than the equivalent horizontal eddies.

Spills

A spill was defined as a rotation of the head, from the snout to the posterior edge of the operculum, of greater than 45 deg followed by downstream body translation of >0.5 body lengths and hence a displacement representing a loss of posture control and location. Spills were not observed for fish swimming in the control, small cylinder or medium cylinder treatments. In the LV treatment, 16 smaller body rotations were observed followed by unidirectional tail flips that did not result in large downstream displacements. These were considered to be displacements that were within the re-stabilizing capability of the fish and hence were not included among the spills.

Spills in turbulent flow created by the two orientations of large cylinders differed in their frequency, with 77 spills occurring in the LH treatment and 31 spills with the LV treatment. In addition, recovery behavior differed with orientation for the large cylinder treatments. For the LV cylinder array treatment, spills and recovery typically followed the sequence given below (Fig. 8).

(1) Rapid body yawing rotation of the head and the start of downstream body translation.

(2) Bending of the body so that the caudal fin subtended an angle near perpendicular to the mean stream flow direction along with simultaneous deployment of the pectoral fin on the same side as the body bend.

(3) Rapid lateral movement of the caudal fin, ending with the body aligned with the local flow.

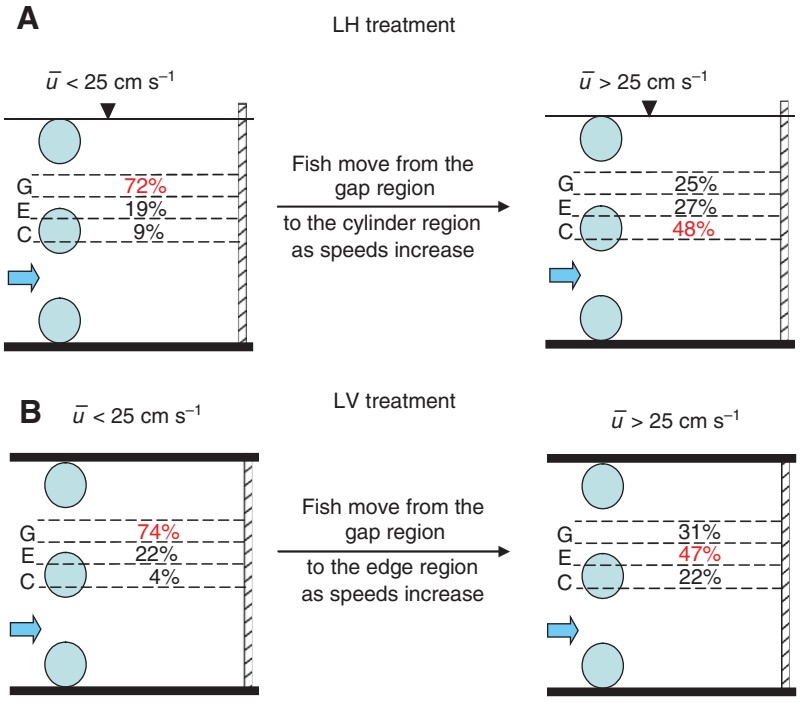

Fig. 7. Flow region preference. (A) Preference downstream from the large horizontal (LH) cylinders. Fish moved from the gap region into the cylinder region with increased $\bar{u}$ (ANCOVA, $P<0.05$ for transverse regions and $\bar{u}$). (B) Preference downstream from the large vertical (LV) cylinders. Fish moved from the gap region into the edge region with increased $\bar{u}$ (ANCOVA, $P<0.05$ for transverse regions and $\bar{u}$). Preferences have been compiled for all flows less than 25 cm s^{-1} (left column) and for all flows greater than 25 cm s^{-1} (right column). The largest percentage in each figure has been highlighted in red. G, the gap region between two cylinders; E, the region at the edge of a cylinder; C, the region directly downstream from a cylinder.

(4) Retraction of the pectoral fins.

(5) Resumption of steady swimming.

Spills and recoveries with the LV cylinder array lasted 410±40 ms.

Spills and recovery in the LH cylinder array treatment followed the same sequence as that of the LV cylinder but with the addition of two body rolls that oriented the caudal fin to counter the pitching moment of the flow perturbation, as given below.

(1) Rapid body pitching rotation of the head and the start of downstream body translation.

(2) A 90 deg body roll such that the fish dorso-ventral axis was horizontal.

(3) Bending of the body so that the caudal fin subtended an angle near perpendicular to the mean stream flow direction and simultaneous deployment of the pectoral fin on the same side as the body bend.

(4) Rapid lateral (vertical) movement of the caudal fin, ending with the body aligned with the local flow.

(5) Retraction of the pectoral fins.

(6) A 90 deg body roll returning the dorso-ventral axis of the body to the horizontal plane.

(7) Resumption of steady swimming.

Spill and recovery in the LH cylinder array treatment lasted 510±40 ms, significantly longer than for the LV treatment (*t*-test, $P<0.05$).

Spills in the presence of large cylinders were observed at all $\bar{u}$ above 28 cm s^{-1} with the speed of first spill averaging 44±3 cm s^{-1} for fish swimming with the LV cylinder array, significantly higher than the 37±1 cm s^{-1} with the LH treatment (*t*-test, $P<0.05$) (Swanson et al., 1998; Maxwell and Delaney, 2004) (Fig. 9). Therefore the control system was overwhelmed in the presence of large horizontal eddies at lower speeds than in the presence of large vertical eddies. Downstream from the LH cylinders fish spent the most time directly behind the cylinders but spilled most frequently in the edge region where the eddies were largest (Fig. 10). Interestingly, downstream from the LV cylinders fish were most often observed in the edge region (52% of the time), nearly twice the preference for this region compared with the LH cylinders. In spite of this doubling of occupation time compared with the LH cylinders, the rate of observed spills was less at 45% of all spills compared with 83% of all spills downstream from the LH cylinders. The strong inability of fish to maintain posture in the LH edge regions compared with the LV edge

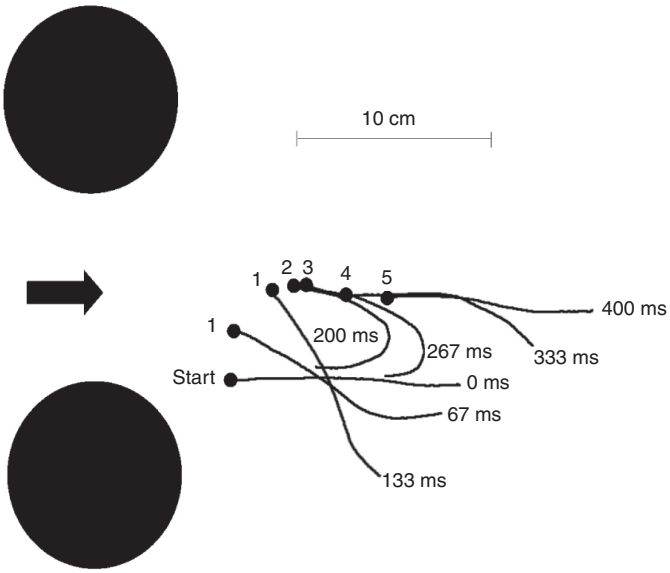

Fig. 8. The body centerline is plotted across 67 ms time steps for a representative spill and recovery. Each line represents the centerline of the fish at Δt=67 ms intervals. Circles indicate the fish head, flow is from left to right on the page. Spills were defined as head rotations greater than 45 deg (t=133 ms) and downstream translation of at least half a body length (t=400 ms). This spill occurred behind the large vertical cylinders at $\bar{u}$=35.1 cm s^{-1} – spill patterns were similar in large horizontal cylinder cases with the addition of two rolls to allow for the tail to be used as a control surface in the appropriate plane. Numbers 1–5 represent each stage of the spill and recovery discussed in the text.

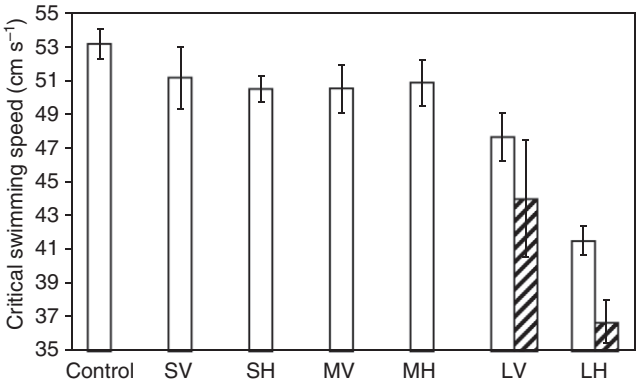

Fig. 9. The critical swimming speed (open bars) and speed of first spill (hatched bars) varied across treatment. The bars represent the mean while the whiskers represent ±2 s.e.m. Spills (defined as head rotations followed by downstream body translation, see Fig. 8) were not observed for fish swimming in the control, small cylinder or medium cylinder array treatments. SV, MV, LV – small, medium and large vertical; SH, MH, LH – small, medium and large horizontal.

regions indicates that eddy orientation is a strong factor in determining the effects of turbulence on the swimming capacity of creek chub.

Critical swimming speed

The 2 min u_{crit} of the creek chub swimming for the control treatment was 53.2±1.8 cm s^{-1} (mean ± 2 s.e.m.) (Fig. 9). Values were significantly lower than the control for all cylinder treatments, the reduction in the 2 min u_{crit} being decreased by 5% within the SH treatment and by 22% within the LH treatment (one-way ANOVA with repeated measures, P<0.05) (Swanson et al., 1998; Maxwell and Delaney, 2004). There was an exception for the SV treatment in which a 5% reduction in 2 min u_{crit} did not prove significant (ANOVA, P=0.063). The 2 min u_{crit} values for the SV, SH, MV and MH treatments were not significantly different from each other (one-way ANOVA with repeated measures, P>0.05) indicating that for the small and medium cylinder treatments there was no cylinder size or orientation effect. The 2 min u_{crit} for fish swimming directly downstream from the large cylinder vertical array was 10% lower than that for the control treatment and was significantly less than the 2 min u_{crit} for the small and medium cylinder treatments (multiple matched pairs t-tests, P<0.05). The 2 min u_{crit} in the LV region was, however, significantly larger than the critical swimming speed for the LH treatment (total reduction in critical swimming speed from the control treatment of 22%, one-way ANOVA with repeated measures, P<0.05). Thus both cylinder diameter and large cylinder orientation significantly affected the critical swimming speed (Fig. 9).

DISCUSSION

Spills occurred only in the presence of large cylinders, which created eddies with large diameters similar to the fish length. Spills occurred relatively rarely with 108 spills on average lasting 483 ms from initiation to recovery. This represented 0.5% of the total swimming time within the large cylinder treatments indicating that it was the relatively large infrequent eddies in the flow that resulted in body displacements. Further, spills were not observed in the large cylinder treatments until velocities were increased to 28 cm s^{-1} (2.3 body lengths s^{-1}).

Spills started with a rapid head rotation followed by downstream translation. The primary axis of head and then body rotation during spills was consistent with the primary eddy orientation (horizontal cylinders resulted in pitching displacements and vertical cylinders resulted in yawing displacements). The angular momentum transferred to the fish from the eddy is therefore assumed to have resulted in a body rotation that was not countered by the fish until after a body rotation of 45 deg occurred. Webb (Webb, 2004a) showed that the yawing and pitching response latency of creek chub is 123±19 ms, which coincides well with our observation that active deployment of fins occurred approximately five video images (133 ms) after initiation of body rotation. In all of the spills analyzed, fin deployment was not initiated until after a 45 deg body rotation occurred.

These observations agree well with previous ideas (Pavlov et al., 2000; Cada and Odeh, 2001; Lupandin, 2005) that eddies of a similar diameter to the fish length provide stability challenges to swimming fish. Lupandin inferred eddy length scales from the autocorrelation of point measurements; however, our results are the first to explicitly show the theorized connection between eddy diameter and stability.

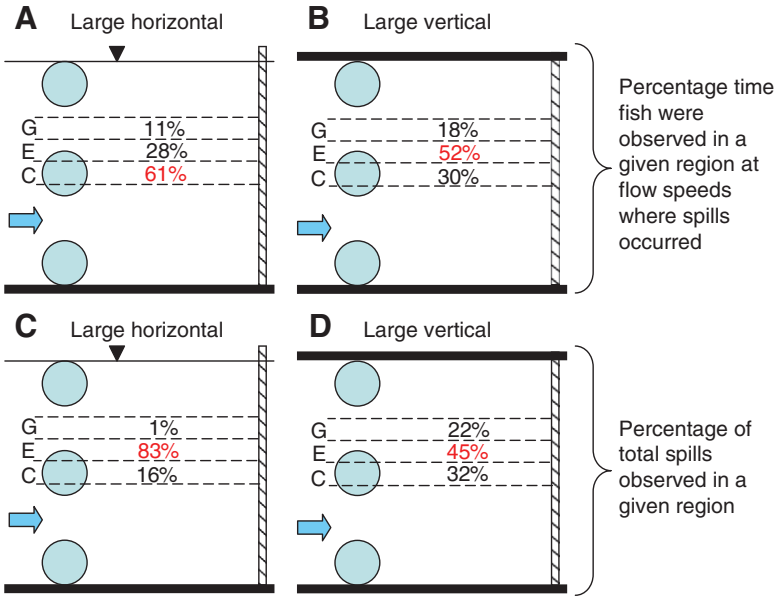

Fig. 10. The percentage time fish occupied a region (A and B) and the percentage of total spills in a region (C and D) for velocities at which spills occurred. (A) Large horizontal and (B) large vertical values represent the mean percentage time spent in a section across all fish for $\bar{u}$ where spills were observed to occur (>28 cm s^{-1}). (C) Large horizontal and (D) large vertical values represent the mean percentage of all spills that occurred in a section across all fish. The largest percentage in each figure has been highlighted in red. G, the gap region between two cylinders; E, the region at the edge of a cylinder; C, the region directly downstream from a cylinder.

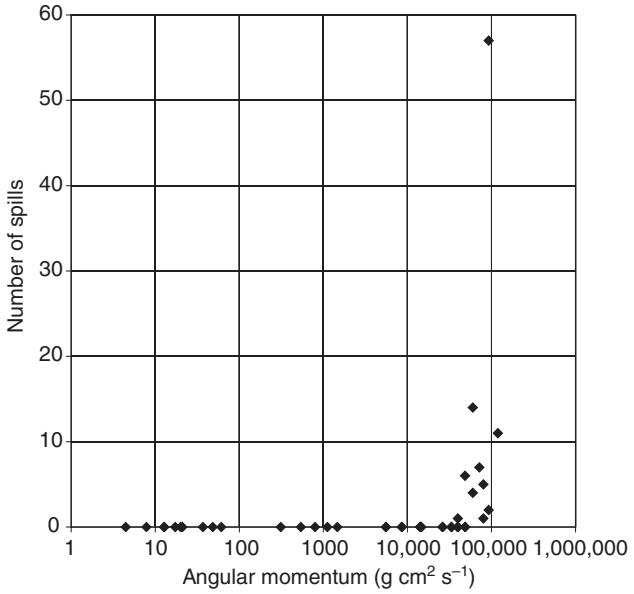

Fig. 11. Number of observed spills as a function of eddy angular momentum. No spills were observed for flows where the angular momentum of the 95th percentile eddy was less than 30,000 g cm^2 s^{-1}.

While large eddies of similar diameter to the fish length create stability challenges, the basis for such challenges cannot rest on diameter alone. For instance, a large eddy with a very slow rotational velocity, as was created downstream from the large cylinders at the lowest velocities, would have a large moment of inertia but would only carry a moderate angular momentum because the eddies are not rotating at a high rate. Under these low velocity/vorticity scenarios no fish spills were observed. The angular velocity, or vorticity, of the eddy is therefore also important in determining the degree to which turbulence affects stability. Higher vorticity leads to greater stability challenges.

An eddy impinging on a fish is associated with a change in momentum (and hence a force) that may cause translational and/or rotational displacements of the fish. The exact displacement of the fish in an eddy–fish interaction will depend upon variables such as the location and duration of interaction, the path of the eddy and the fish during impact, and stabilizing behaviors by the fish that are difficult to quantify and generalize. However, whether an eddy has the potential to destabilize a swimming fish should be a function of the maximum angular momentum of the eddy. The larger the angular momentum of an eddy, the greater the likelihood that a fish–eddy interaction will result in a loss of stability for the fish. The maximum angular momentum of the eddy, Π_e, is given by:

$$\Pi_e = \frac{m_e \Gamma_e}{4\pi} , \quad (3)$$

where m_e is the eddy mass (Tennekes and Lumley, 1972; Saffman, 1992). The eddy mass is calculated as:

$$m_e = \rho_w \forall_e , \quad (4)$$

where ρ_w is the water density and $\forall_e$ is the eddy volume. Following the 'vortex string' conceptualization of eddies – that eddies are long rotating bodies of fluid (Pullin and Saffman, 1998) – the eddy volume can be calculated as:

$$\forall_e = a_e L_e , \quad (5)$$

where a_e is the eddy area ($0.25\pi d_e^2$) and L_e is the eddy length. Williamson (Williamson, 1996) showed that for the Reynolds numbers found in these experiments, Re=340–45,000, three-dimensional instabilities tend to break up vortex strings into lengths of the order of their diameter. The angular momentum of eddies was therefore calculated as:

$$\Pi_e = \frac{\pi}{64} \rho_w \omega_e d_e^5 . \quad (6)$$

The flows where spills did occur were composed of eddies with angular momentum (Ω_e) greater than 30,000 g cm^2 s^{-1} (Fig. 11). Above this value the rate of spills also increased with eddy angular momentum.

Spills occurred when the self-correcting and powered stabilizing capacity of the body and fins was exceeded (Webb and Weihs, 1994; Lauder and Jayne, 1996; Webb, 2002; Webb, 2004b). The present observations provide support to earlier postulations that the stabilizing control system of fish such as creek chub (with fin pattern and body geometry common to fluvial fishes) would be better suited for countering yawing rather than pitching perturbations (Harris, 1936; Harris, 1938; Aleyev, 1977; Fish and Shannahan, 2000; Weihs, 2002; Fish, 2002; Webb, 1998; Webb, 2006). In addition, similarities have been noted between functional morphological features and maneuverability in various directions depending upon body depth, body compression and fin placement (Howland 1974; Webb et al., 1996; Schrank et al., 1999; Drucker and Lauder, 2001).

Once spills occur, rapid recovery becomes important in order to both minimize the risk of injury and reduce energy requirements to regain location. The caudal fin, with fast-start types of body–fin motions, was used to recover from both yawing and pitching displacements. These types of body motions are known to create the largest propulsive forces (Domenici and Blake, 1997; Hale, 1999) associated with the largest area, span, amplitude and moment arm (Weihs, 1972; Weihs, 1973; Webb et al., 1991). However, the caudal fin is oriented in the lateral plane for most fishes, and therefore can only create large torques to correct yawing displacements. In order to utilize this fin for recovery from pitching spills, the fin had to be rotated into the vertical plane. This was achieved by rolling the body 90 deg. Similar behavior has been reported previously (Webb et al., 1996; Schrank et al., 1999) in goldfish (*Carassius auratus*), angelfish (*Pterophyllum scalare*) and silver dollars (*Metynnis hypsauchen*) maneuvering through horizontal slits and bent tubes. Similarly, cetaceans combine rolling and rotation of the caudal peduncle to rotate the normally horizontal tail fluke into the vertical plane to execute yawing turns (Fish, 2002; Rohr and Fish, 2004). The addition of two rolls in recovery maneuvers by creek chub increased recovery time by 24% for horizontal *versus* vertical spills.

The medium and small cylinder arrays resulted in a 5% reduction in the 2 min u_{crit} compared with the control. Tests of fish swimming in the LV and LH cylinder arrays resulted in a 10% and 22% reduction in the critical swimming speed, respectively, compared with the control. These values were both significantly different from the control and significantly different from each other (ANOVA, P<0.05). Presumably there were energy costs associated with recovery maneuvers that contributed to lower critical swimming speeds. While the pattern of spills provides the most insight into the limits of stability control in the presence of large eddies, the reduction in critical swimming speed when spills became more common attests to the general deleterious impacts of large eddies for overall swimming performance. The greater reduction in the 2 min u_{crit} for the large

horizontal cylinder array further supports the observations on spill, showing that pitching perturbations in the flow present larger challenges than yawing perturbations.

CONCLUSIONS

A series of increasing velocity tests were conducted to determine the influence of turbulent eddies on the critical swimming speed and stability of creek chub. Eddy vorticity, eddy diameter and eddy orientation (spinning about horizontal or vertical axes of rotation) were varied using arrays of cylinders 0.4, 1.6 and 8.9 cm in diameter. The occurrence of spills (defined as rapid head rotations followed by downstream translation) increased with increasing eddy angular momentum. Furthermore the greatest reduction in the 2 min u_{crit} of fish occurred in the large cylinder flow treatments, where the vorticity, diameter and angular momentum were greatest. Because eddy angular momentum is a function of the eddy diameter and eddy vorticity, these results confirm the importance of turbulence scale (based on eddy diameter with respect to the fish length) and vorticity proposed by other researchers (e.g. Pavlov et al., 2000; Cada and Odeh, 2001; Lupandin, 2005; Liao, 2007).

The 2 min u_{crit} was affected by the orientation of cylinder arrays for the large cylinder treatment, being reduced 10±4% compared with the control treatment with the vertical array and by 22±3% for the horizontal array. This orientation effect for the large cylinders was investigated through video analysis of the fish spills. Spills occurred 230% more frequently in turbulent flow fields dominated by large horizontal eddies than in turbulent flow fields dominated by large vertical eddies. Recovery from a spill took 24% more time for fish in the horizontal turbulent eddy field compared with the vertical turbulent eddy field. The increased recovery time was due to two additional rolls which rotated the caudal fin into the plane of the displacement.

These results shed further light on the importance of turbulence on the swimming ability of fish in a fluvial environment. In turbulent fluvial environments fish are forced to cope with the same destabilizing forces produced in these experiments. The results of these experiments suggest that habitat selection, station holding, migration and ability to maintain posture in a flow will be affected by the presence of turbulent eddies in the close vicinity of fish. Specifically, eddies that are horizontal in orientation, rotate rapidly and have a diameter approximately equal to the fish length are expected to cause the greatest stability challenges for a free swimming fish. The general conclusions as to the importance of eddy diameter, vorticity, angular momentum and orientation have the potential to improve future fishway and stream restoration designs.

These results derive from a limited number of individuals all of the same species, of the same length and from the same reach of river. While variability across individuals was low in this experiment, prior to globalizing the trends, future tests should expand this work across species, life stage and body/fin morphology.

ACKNOWLEDGEMENTS

This work was submitted in partial fulfillment for the Degree of Doctor of Philosophy at the University of Michigan. This work was supported in part by grants to A.J.C. and Dr P. W. Webb (Sea Grant R/GLF-53) and to A.J.C. (NSF Career CTS-0447427). Partial support to H.M.T. was also provided through Alumni Scholarship from the School of Natural Resources and Environment, and a pre-doctoral fellowship from the Rackham School of Graduate Studies at the University of Michigan. We are grateful to Dr Paul Webb for his feedback throughout this project.

REFERENCES

Akilli, H., Akar, A. and Karakus, C. (2004). Flow characteristics of circular cylinders arranged side-by-side in shallow water. *Flow Meas. Instrument.* **15**, 187-197.
Aleyev. Y. G. (1977). *Nekton.* The Hague: Junk.
Batchelor, G. K. and Townsend, A. A. (1947). Decay of vorticity in isotropic turbulence. *Proc. R. Soc. Lond. Ser. A* **190**, 534-550.
Biggs, B. J. F., Nikora, V. I. and Snelder, T. H. (2005). Linking Scales of flow variability to lotic ecosystem structure and function. *River Res. Applications* **21**, 283-298.
Brett, J. R. (1963). Energy required for swimming by young sockeye salmon with a comparison of drag force on a dead fish. *Trans. R. Soc. Can.* **1**, 441.
Cada, G. F. and Odeh, M. (2001). Turbulence at hydroelectric power plants and its potential effects on fish. *Report to Bonneville Power Administration*, Contract No. 2000AI26531, Project No. 200005700: 1-37.
Cimbala, J. M., Nagib, H. M. and Roshko, A. (1988). Large structure in the far wakes of two-dimensional large bodies. *J. Fluid Mech.* **190**, 265-298.
Cotel, A. J., Webb, P. W. and Tritico, H. M. (2006). Do brown trout choose locations with reduced turbulence? *Trans. Am. Fish. Soc.* **135**, 610-619.
Domenici, P. and Blake, R. W. (1997). The kinematics and performance of fish fast-start swimming. *J. Exp. Biol.* **200**, 1165-1178.
Drucker, E. G. and Lauder, G. V. (1999). Locomotor forces on a swimming fish: three-dimensional vortex wake dynamics quantified using digital particle image velocimetry. *J. Exp. Biol.* **202**, 2393-2412.
Drucker, E. G. and Lauder, G. V. (2001). Wake dynamics and fluid forces of turning maneuvers in sunfish. *J. Exp. Biol.* **204**, 431-442.
Enders, E. C., Boisclair, D. and Roy, A. G. (2003). The effect of turbulence on the cost of swimming for juvenile atlantic salmon. *Can. J. Fish. Aquat. Sci.* **60**, 1149-1160.
Farlinger, S. and Beamish, F. W. H. (1977). Effects of time and velocity increments in the critical swimming speeds of largemouth bass (*Micropterus salmoides*). *Trans. Am. Fish. Soc.* **106**, 436-439.
Fish, F. E. (2002). Balancing requirements for stability and maneuverability in cetaceans. *Integr. Comp. Biol.* **42**, 85-93.
Fish, F. E. and Shannahan, L. D. (2000). The role of the pectoral fins in body trim of sharks. *J. Fish Biol.* **56**, 1062-1073.
General Pixels (2000). *PixelFlow 2.1 Installation and User's Guide.* Pasadena, CA, USA: General Pixels.
Gharib, M. and Dabiri, D. (2000). An overview of digital particle image velocimetry. In *Flow Visualization: Techniques and Examples* (ed. A. Smits and T. T. Lim). London: Imperial College Press.
Hale, M. E. (1999). Effects of size and ontogeny on the fast-start performance of several salmonid species. *J. Exp. Biol.* **202**, 1465-1479.
Harris, J. E. (1936). The role of fins in the equilibrium of swimming fish. I. Wind-tunnel tests on a model of *Mustelus canis* (Mitchell). *J. Exp. Biol.* **13**, 476-493.
Harris, J. E. (1938). The role of the fins in the equilibrium of swimming fish II. The role of the pelvic fins. *J. Exp. Biol.* **15**, 32-47.
Howland, H. C. (1974). Optimal strategies for predator avoidance: the relative importance of speed and manoeuverability. *J. Theor. Biol.* **47**, 333-350.
Huang, H., Dabiri, D. and Gharib, M. (1997). On errors of digital particle image velocimetry. *Meas. Sci. Technol.* **8**, 1427-1440.
Landry, F., Miller, T. J. and Leggett, W. C. (1995). The effects of small-scale turbulence on the ingestion rate of fathead minnow larvae. *Can. J. Fish. Aquat. Sci.* **52**, 1714-1719.
Lauder, G. V. and Jayne, B. C. (1996). Pectoral fin locomotion in fishes: testing drag-based models using three-dimensional kinematics. *Am. Zool.* **36**, 567-581.
Liao, J. C. (2007). A review of fish swimming mechanics and behavior in altered flows. *Philos. Trans. R. Soc. Lond. B. Biol. Sci.* **362**, 1973-1993.
Liao, J. C., Beal, D. N., Lauder, G. V. and Triantafyllou, M. S. (2003). The Karman gait: novel body kinematics of rainbow trout swimming in a vortex street. *J. Exp. Biol.* **206**, 1059-1073.
Lupandin, A. I. (2005). Effect of flow turbulence on swimming speed of fish. *Biol. Bull.* **32**, 558-565.
Mackenzie, B. R. and Kiorboe, T. (1995). Encounter rates and swimming behavior of pause-travel and cruise larval fish predators in calm and turbulent laboratory environments. *Limnol. Oceanogr.* **40**, 1278-1289.
Mackenzie, B. R. and Kiorboe, T. (2000). Larval fish feeding and turbulence: a case for the downside. *Limnol. Oceanogr.* **45**, 1-10.
Mackenzie, B. R., Miller, T. J., Cyr, S. and Leggett, W. C. (1994). Evidence for a dome shaped relationship between turbulence and larval fish ingestion rates. *Limnol. Oceanogr.* **39**, 1790-1799.
Maxwell, S. E. and Delaney, H. D. (2004). *Designing Experiments and Analyzing Data*, 2nd Edn. Mahwah, NJ: Lawrence Erlbaum Associates, Inc.
Montgomery, D. R., Buffington, J. M., Peterson, N. P., Schuett-Hames, D. and Quin, T. P. (1996). Stream-bed scour, egg burial depths, and the influence of salmonid spawning on bed surface mobility. *Can. J. Fish. Aquat. Sci.* **53**, 1061-1070.
Nikora, V. I. and Goring, D. G. (1998). Effects of bed mobility on turbulence structure. *NIWA Internal Report No 48.* Christchurch, New Zealand: NIWA.
Nikora, V. I., Aberlee, J., Biggs, B. J. F., Jowett, I. G. and Sykes, J. R. E. (2003). Effects of fish size, time to fatigue, and turbulence on swimming performance: a case study of *Galaxias maculatus*. *J. Fish Biol.* **63**, 1365-1382.
Pavlov, D. S., Lupandin, A. I. and Skorobogatov, M. A. (2000). The effects of flow turbulence on the behaviour and distribution of fish. *J. Ichthyol.* **40**, S232-S261.
Pullin, D. I. and Saffman, P. G. (1998). Vortex dynamics in turbulence. *Annu. Rev. Fluid Mech.* **30**, 31-51.
Rohr, J. J. and Fish, F. E. (2004). Strouhal numbers and optimization of swimming by odontocete cetaceans. *J. Exp. Biol.* **207**, 1633-1642.
Roshko, A. (1976). Structure of turbulent shear flows: a new look. *AIAA J.* **14**, 1349-1357.
Saffman, P. G. (1992). *Vortex Dynamics.* Cambridge: Cambridge University Press.
Schrank, A. J., Webb, P. W. and Mayberry, S. (1999). How do body and paired-fin positions affect the ability of three teleost fishes to maneuver around bends? *Can. J. Zool.* **77**, 203-210.

Smith, D. L., Brannon, E. L. and Odeh, M. (2005). Response of juvenile rainbow trout to turbulence produced by prismatoidal shapes. *Trans. Am. Fish. Soc.* **134**, 741-753.
Standen, E. M., Hinch, S. G., Healey, M. C. and Farrell, A. P. (2002). Energetic costs of migration through the Fraser River Canon, British Columbia, in adult pink and sockeye salmon as assessed by EMG Telemetry. *Can. J. Fish. Aquat. Sci.* **59**, 1809-1818.
Standen, E. M., Hinch, S. G. and Rand, P. S. (2004). Influence of river speed on path selection by migrating adult sockeye salmon. *Can. J. Fish. Aquat. Sci.* **61**, 905-912.
Swanson, C., Paciencia, S. Y. and Cech, J. J. (1998). Swimming performance of delta smelt: maximum performance and behavioral kinematic limitations on swimming at submaximal velocities. *J. Exp. Biol.* **201**, 333-345.
Taylor, G. I. (1938). Production and dissipation of vorticity in a turbulent fluid. *Proc. R. Soc. Lond. Ser. A* **164**, 15-23.
Tennekes, H. and Lumley, J. L. (1972). *A First Course in Turbulence*. Cambridge, MA: The MIT Press.
Tritico, H. M. (2009). The effects of turbulence on habitat selection and swimming kinematics of fishes. Dissertation submitted in partial fulfillment of the requirements for the degree of doctor of philosophy, University of Michigan Ann Arbor.
Tritico, H. M. and Hotchkiss, R. H. (2005). Unobstructed and obstructed turbulent flow in gravel bed rivers. *J. Hydraulic Eng.* **131**, 635-645.
Tritico, H. M., Cotel, A. J. and Clarke, J. N. (2007). Development, testing and demonstration of a portable submersible miniature particle imaging velocimetry device. *Meas. Sci. Technol.* **18**, 2555-2562.
Von Karman, T. (1937). The fundamentals of the statistical theory of turbulence. *J. Aero. Sci.* **4**, 131-138.
Webb, P. W. (1998). Entrainment by river chub *Nocomis micropogon* and smallmouth bass *Micropterus dolomieu* on cylinders. *J. Exp. Biol.* **201**, 2403-2412.
Webb, P. W. (2002). Control of posture, depth, and swimming trajectories of fishes. *Integr. Comp. Biol.* **42**, 94-101.
Webb, P. W. (2004a). Response latencies to postural disturbances in three species of teleostean fishes. *J. Exp. Biol.* **207**, 955-961.
Webb, P. W. (2004b). Maneuverability – General Issues. *IEEE J. Oceanic Eng.* **29**, 547-555.
Webb, P. W. (2006). Stability and maneuverability. In *Fish Physiology* (ed. R. E. Shadwick and G. V. Lauder), pp. 281-332. San Diego: Elsevier Press.
Webb, P. W. and Weihs, D. (1994). Hydrostatic stability of fish with swimbladders: Not all fish are unstable. *Can. J. Zool.* **72**, 1149-1154.
Webb, P. W., Kostecki, P. T. and Stevens, E. D. (1984). The effect of size and swimming speed on locomotor kinematics of rainbow trout. *J. Exp. Biol.* **109**, 77-95.
Webb, P. W., Sims, D. and Schultz, W. W. (1991). The effect of an air/water interface on the faststart performance of rainbow trout (*Oncorhynchus mykiss*). *J. Exp. Biol.* **155**, 219-226.
Webb, P. W., LaLiberte, G. D. and Schrank, A. J. (1996). Does body and fin form affect the maneuverability of fish traversing vertical and horizontal slits? *Environ. Biol. Fishes.* **46**, 7-14.
Weihs, D. (1972). A hydrodynamical analysis of fish turning manoeuvres. *Proc. R. Soc. Lond. B. Biol. Sci.* **182**, 59-72.
Weihs, D. (1973). The mechanism of rapid starting of slender fish. *Biorheology* **10**, 343-350.
Weihs, D. (2002). Stability versus maneuverability in aquatic locomotion. *Integr. Comp. Biol.* **42**, 127-134.
Westerweel, J., Dabiri, D. and Gharib, M. (1997). The effect of a discrete window offset on the accuracy of cross-correlation analysis of digital PIV recordings. *Exp. Fluids* **23**, 20-28.
Wilga, C. D. and Lauder, G. V. (1999). Locomotion in sturgeon: function of the pectoral fins. *J. Exp. Biol.* **202**, 2413-2432.
Wilga, C. D. and Lauder, G. V. (2002). Function of the heterocercal tail in sharks: quantitative wake dynamics during steady horizontal swimming and vertical maneuvering. *J. Exp. Biol.* **205**, 2365-2374.
Williamson, C. H. K. (1996). Vortex dynamics in the cylinder wake. *Annu. Rev. Fluid Mech.* **28**, 477-539.
Zdravkovich, M. M. (2003). *Flow around Circular Cylinders Vol. 2, Applications*. Oxford, UK: Oxford University Press.
Zhang, H. J. and Zhou, Y. (2001). Effect of unequal cylinder spacing on vortex streets behind three side-by-side cylinders. *Phys. Fluids* **13**, 3675-3686.